Journal of Catalysis 268 (2009) 384–389

Contents lists available at ScienceDirect

Journal of Catalysis

journal homepage: www.elsevier.com/locate/jcat

Research Note

# On the mechanism of hydrogen-promoted gold-catalyzed CO oxidation

Elodie Quinet [a], Laurent Piccolo [a,*], Franck Morfin [a], Priscilla Avenier [b], Fabrice Diehl [b], Valérie Caps [a,1], Jean-Luc Rousset [a]

[a] Université Lyon 1, CNRS, UMR 5256, IRCELYON, Institut de Recherches sur la Catalyse et l'Environnement de Lyon, 2 Avenue Albert Einstein, F-69626 Villeurbanne, France
[b] IFP Lyon, BP no. 3, 69360 Solaize, France

ARTICLE INFO

*Article history:*
Received 2 August 2009
Revised 21 September 2009
Accepted 23 September 2009
Available online 22 October 2009

*Keywords:*
CO oxidation
PrOx or SelOx
Hydrogen
Gold
Hydroperoxy intermediates

ABSTRACT

The kinetics of CO oxidation, $H_2$ oxidation and preferential CO oxidation (PrOx) over $Au/Al_2O_3$ catalysts have been investigated. The catalysts with the smallest particles (~2 nm) are the most active for all three reactions. As previously observed, the presence of $H_2$ greatly promotes CO oxidation, which becomes faster than CO-free $H_2$ oxidation at low temperature. From these results and on the basis of previous works, we propose a complete PrOx mechanism. The reaction involves Au–OOH, Au–OH and Au–H intermediates, also involved in $H_2$ oxidation, and benefits from the presence of low-coordination sites.



## 1. Introduction

CO oxidation and preferential oxidation (PrOx) of CO in the presence of hydrogen are important reactions for pollution control and energy production [1,2]. In addition, low-temperature CO oxidation has served as a prototypical reaction in catalysis by gold [3–5]. In particular, it has been used as a test-reaction to investigate the mechanisms of oxygen activation that proceeds in a more complex way on gold than over group 8 metals. On these metals, the classical Langmuir–Hinshelwood mechanism applies, for which $O_2$ dissociates at the surface prior to reaction between atomic oxygen and molecular CO [6]. For oxide-supported gold nanoparticles, while CO is known to adsorb on gold atoms [3], several classes of active sites have been suggested for oxygen activation: interfacial metal-oxide sites, cationic gold sites, low-coordination gold atoms, etc. [7].

In the course of our investigation of gold-catalyzed PrOx, we have focused on the effect of $H_2$ addition on CO oxidation. We have demonstrated that the CO oxidation pathway is strongly modified in the presence of $H_2$ [8]. Indeed, even a low $H_2$ amount added to a $CO + O_2$ feed appears to accelerate CO oxidation. The extent of the $H_2$-induced promotion is particularly spectacular for catalysts such as $Au/Al_2O_3$, in which the supports are poorly efficient for oxygen activation [8–11]. The $Au/Al_2O_3$ system is thus relevant for studying $H_2$ effects. Over the $Au/TiO_2$ catalyst, which is anyway very active in $H_2$-free CO oxidation, the promotion by $H_2$ (similarly to that by water [12]) is weaker; it either regenerates the catalyst [13,14] or slightly promotes its activity [15,16].

Based on kinetic, spectroscopic and theoretical works [8,11,17–19], we have suggested that the simultaneous presence of $O_2$ and $H_2$ on gold-based materials may stabilize $Au–O_xH_y$ species (e.g., Au–OOH), which would in turn efficiently react with CO to form $CO_2$. We have recently reinforced this hypothesis by identifying the O–H vibration by *operando* infrared spectroscopy (DRIFTS) on both $Au/TiO_2$ [15] and *unsupported gold*, which also catalyzes the promotion of CO oxidation by $H_2$ [20].

In this article, we provide new kinetic data, which help us to correlate the PrOx activity to the $H_2$ oxidation activity. These results support the involvement of hydroperoxy species in PrOx and lead us to propose a detailed reaction scheme for $H_2$-promoted CO oxidation.

## 2. Experimental

The alumina-supported gold catalysts were synthesized by direct anionic exchange (DAE) [21] or colloidal deposition (CD) [22,23]. In DAE, a $1.4 \times 10^{-4}$ mol $L^{-1}$ $HAuCl_4$ (Alfa-Aesar, 99.99%) aqueous solution was prepared and added to 1 g of alumina powder (Axens). The solution was heated to 70 °C and was either stirred for 1 h and *ex situ* washed (AE-ex) or stirred for 20 min and *in situ* washed (AE-in) in order to remove residual chlorine that favours sintering [24]. In *ex situ* washing, the slurry was filtered

* Corresponding author. Fax: +33 472445399.
*E-mail address:* laurent.piccolo@ircelyon.univ-lyon1.fr (L. Piccolo).
[1] Present address: KAUST Catalysis Center (KCC), 4700 King Abdullah University of Science and Technology, Thuwal 23955 – 6900, Saudi Arabia.

0021-9517/$ - see front matter © 2009 Elsevier Inc. All rights reserved.
doi:10.1016/j.jcat.2009.09.019

and the catalyst was suspended in dilute ammonia (0.17 mol $L^{-1}$) and was filtered again. Alternatively, the slurry was mixed with concentrated ammonia (Merck, 17 mol $L^{-1}$), and was filtered after 20 min (*in situ* washing). Finally, the catalyst was dried in air at 120 °C overnight and calcined in air at 300 °C for 4 h (heating ramp 5 °C/min). In CD, 0.3 mL of a 0.25 mol $L^{-1}$ $HAuCl_4$ solution was added to 100 mL of water. After stirring for 5 min, a 1.3 mL solution of polyvinyl alcohol (0.5 wt.%, obtained by diluting PVA Mw 10,000 from Aldrich in distilled water) was added, followed by the addition of 2.5 mL of $NaBH_4$ (0.1 mol $L^{-1}$) after 10 min. Then 1 g of alumina powder was added to the solution. After 24 h of deposition, the mixture was filtered and *ex situ* washed for 1 h with diluted ammonia. Finally, the catalyst was dried in air at 120 °C overnight and calcined in air at 300 °C for 4 h (heating ramp 5 °C/min). The $Au/TiO_2$ reference catalyst tested for comparison was purchased from the World Gold Council (Sample A, #53 synthesized by deposition–precipitation) [3,25].

The metal contents of the catalysts were determined by inductively coupled plasma-optical emission spectrometry (ICP-OES, Activa – Horiba Jobin Yvon). The size distribution of gold nanoparticles was determined by high-resolution transmission electron microscopy (HRTEM, Jeol JEM 2010, 0.196 nm point-to-point resolution). For each sample, more than 200 particles over ca. 20 micrographs were counted. The sample characteristics are summarized in Table 1.

Activity measurements were carried out in a continuous flow fixed bed reactor (internal diameter 10 mm) at atmospheric pressure and variable temperature. The catalyst was diluted in the corresponding support (or in Condea Puralox ScFa-215 γ-alumina for $Au/TiO_2$ and AE-0 samples) and the catalytic bed height in the quartz tube reactor was 13 mm. The reactant gases (2 vol.% CO and/or 2 vol.% $O_2$ and/or 48 vol.% $H_2$ in standard $H_2$ ox, CO ox and PrOx experiments, see Fig. 1; see Table 2 for non-standard conditions), balanced in helium, were sent through the reactor at a total flow rate of 50 mL $min^{-1}$. The outlet gases were analyzed online with a Varian-Micro GC (CP2003) equipped with a TCD detector. More details on catalytic testing can be found in Refs. [8,9,11,20].

## 3. Results

Fig. 1 allows us to compare the activities of $Au/Al_2O_3$ catalysts with average particle sizes ranging from 2 to 30 nm, obtained by various methods: colloidal deposition (CD), anionic exchange without washing (AE-0), anionic exchange with *in situ* washing (AE-in) or *ex situ* washing (AE-ex) using $NH_4OH$. An $Au/\delta\text{-}Al_2O_3$ catalyst with 2 nm-sized particles prepared by AE-ex was heated to 500 °C in air, which led to 7 nm-sized particles (see Table 1). Commercial $Au/TiO_2$ serves as a reference. The catalytic performances were evaluated through four reactions: CO oxidation without $H_2$ (CO ox, Fig. 1a), $H_2$ oxidation without CO ($H_2$ ox, Fig. 1b), CO oxidation with $H_2$ (CO PrOx, Fig. 1c), and $H_2$ oxidation with CO ($H_2$ PrOx, Fig. 1d).

**Table 1**
Characteristics of the gold catalysts.

| Catalyst | Preparation method[a] | Au loading (wt.%) (ICP) | Surface area ($m^2\ g^{-1}$) (BET) | Particle size (nm) (TEM) |
|---|---|---|---|---|
| $Au/TiO_2$ | DP | 1.4 | 60 | 3.7 ± 1.5 |
| $Au/\delta\text{-}Al_2O_3$ | AE-ex | 1.4 | 140 | 1.9 ± 0.8 |
| $Au/\delta\text{-}Al_2O_3$ | AE-ex | 1.4 | 140 | 6.9 ± 2.3 |
| $Au/\gamma\text{-}Al_2O_3$ | AE-in | 0.77 | 190 | 2.0 ± 0.7 |
| $Au/\gamma\text{-}Al_2O_3$ | AE-0 | 1.3 | 190 | ~26 |
| $Au/\gamma\text{-}Al_2O_3$ | CD | 1.2 | 190 | 4.1 ± 2.1 |

[a] DP: deposition–precipitation (World Gold Council); AE: anionic exchange; CD: colloidal deposition.

Noticeably, whatever the reaction and temperature considered, the order of activity (per gold weight) for $Au/Al_2O_3$ is: 2 nm-sized particles > 4–7 nm-sized particles > 30 nm-sized particles, due to the larger metallic surface exposed on the smaller particles. Catalysts with small particles remain the most efficient ones in terms of turnover frequency (TOF, i.e., rate per surface gold atom, calculated from dispersions determined by TEM), as shown by Table 2 for the $Au/\delta\text{-}Al_2O_3$ catalysts. The size effect is well known in CO oxidation [3,5], for which the particle–support interface plays an important role (see Section 1), and the same size dependency (for particles containing at least 13 Au atoms) has been evidenced for $H_2$ oxidation on $Au/SiO_2$ [17].

To our knowledge, the influence of gold particle size on PrOx is not documented. Actually, except for the reference catalyst, only $Au/\gamma\text{-}Al_2O_3$ (AE-in, 2 nm) and $Au/\delta\text{-}Al_2O_3$ (AE-ex, 2 nm) are highly active in PrOx, even though all the catalysts are promoted at low temperature by the presence of $H_2$. The alumina phase (δ,γ) of the support has only little influence. In the high-temperature region, the CO oxidation rates decrease due to competitive $O_2$ reaction with $H_2$ (to produce water), as also observed for other gold catalysts [8,16]; at this stage, $O_2$ conversion is 100%. The $H_2$ oxidation rates are moderately reduced by the presence of CO (PrOx), especially at low temperature.

The high efficiency of small supported particles in CO PrOx correlates with their high efficiency in $H_2$ oxidation, which in turn is related to particle size ($TOF_{H_2\ ox} = 0.43\ s^{-1}$ for 2 nm-sized particles vs. less than 0.1 $s^{-1}$ for 7 nm-sized particles at 60 °C, see Table 2). Thus, the CO PrOx efficiency of a catalyst appears driven by its ability to activate $H_2$.

Moreover, the promoting effect of $H_2$ increases as gold particle size decreases. Indeed, the CO oxidation rates dramatically increase in the presence of $H_2$ at low temperature for all the catalysts, but to a larger extent for small particles: e.g., at 60 °C, the amplification factor ($TOF_{CO\ PrOx}/TOF_{CO\ ox}$) is ~30 for 2 nm-sized particles (leading to a $TOF_{CO\ PrOx}$ of 0.82 $s^{-1}$) while it is 8 for 7 nm-sized particles ($TOF_{CO\ PrOx} = 0.15\ s^{-1}$) obtained by thermal sintering from the same $Au/\delta\text{-}Al_2O_3$ batch (Table 2).

It is worth noting that $Au/TiO_2$ is more active than all the $Au/Al_2O_3$ catalysts in all the reactions (see Table 2 for TOFs at 60 °C), possibly due to support-dependent particle morphologies and additional support-mediated reaction pathways. However, the difference between $Au/TiO_2$ and the most active $Au/Al_2O_3$ is dramatic in the sole case of CO oxidation (without $H_2$): CO oxidation on $Au/Al_2O_3$ is greatly promoted by $H_2$, whereas CO oxidation on $Au/TiO_2$ is only slightly promoted. Thus, the presence of $H_2$ reduces the influence of the support: a poor CO oxidation catalyst such as $Au/Al_2O_3$ can be an efficient PrOx catalyst.

Considering now the selectivity to $CO_2$ in PrOx (Fig. 1e), one can observe that all the catalysts behave similarly: the selectivity is higher than 90% at temperatures lower than ~40 °C, and decreases gradually when temperature increases, to finally vanish at ~300 °C. This temperature dependence in PrOx selectivity is well known [5] and will be discussed in mechanistic terms later on.

The $Au/\delta\text{-}Al_2O_3$ (AE-ex) catalyst with 2 nm-sized particles has been selected for further kinetic studies. CO ox, CO PrOx, $H_2$ ox and $H_2$ PrOx were studied between room temperature and 280 °C at atmospheric pressure by varying successively the partial pressure of each reactant. The results concerning reaction partial orders are reported in Table 3 (the corresponding plots are shown in Fig. S1, Supplementary material). The effect of variable hydrogen concentrations on $Au/Al_2O_3$ properties has already been published, using 0.92 wt.% $Au/\delta\text{-}Al_2O_3$ (AE-ex, 5.8 ± 2.2 nm) [11], hence we only summarize the new results here. While it is 0.5–0.7 in $H_2$ oxidation (in agreement with calculations from Ref. [17]) and $H_2$ PrOx,

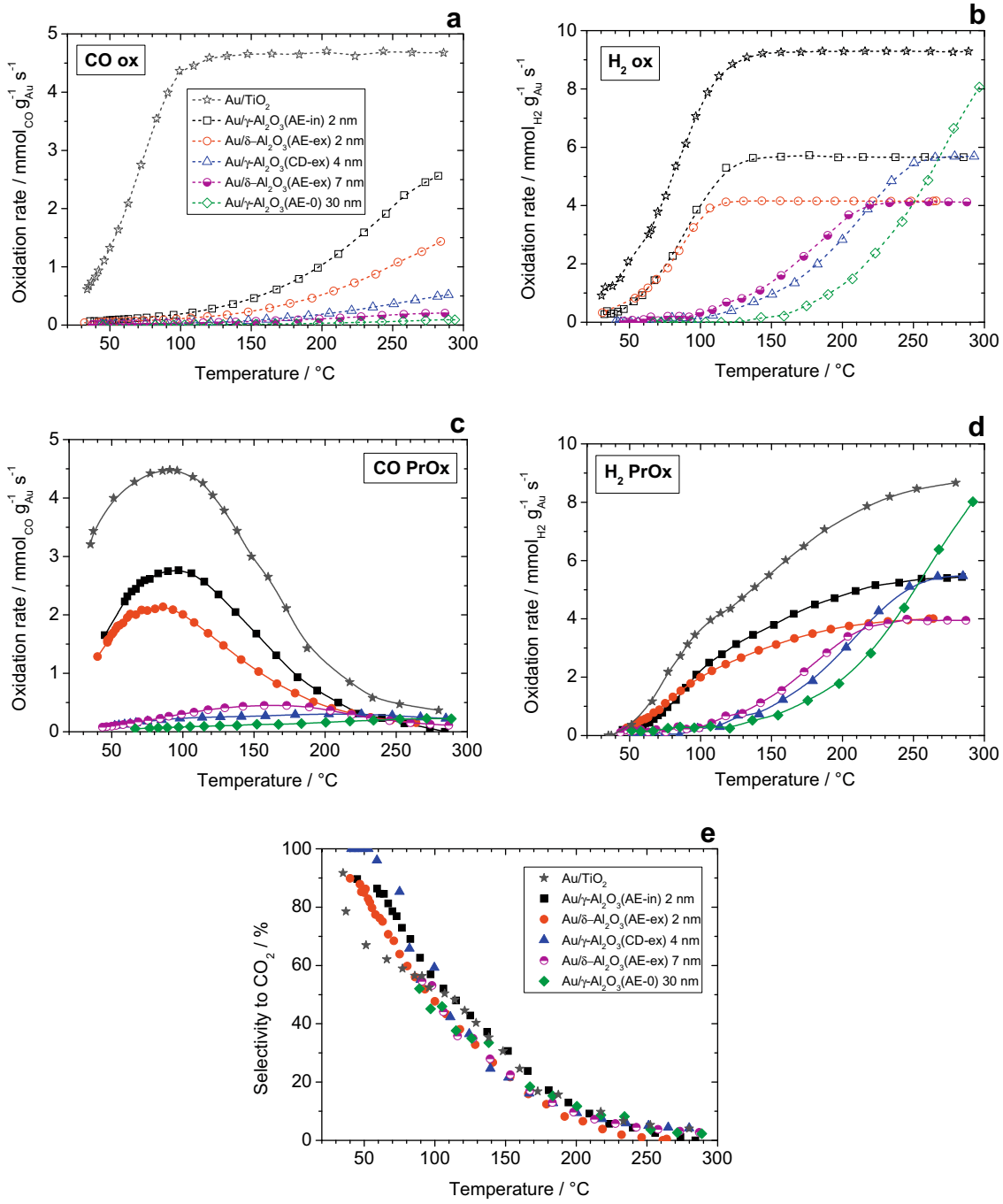


**Fig. 1.** Catalytic performances of $Au/Al_2O_3$ catalysts and reference $Au/TiO_2$. (a) CO oxidation without $H_2$; (b) $H_2$ oxidation without CO; (c) CO preferential oxidation in the presence of $H_2$; (d) $H_2$ preferential oxidation in the presence of CO; (e) selectivity to $CO_2$ in PrOx. Conditions: 2 vol.% CO and/or 2 vol.% $O_2$ and/or 48 vol.% $H_2$ balanced in He. Gold amount: $Au/TiO_2$ 0.16 mg; $Au/\gamma$-$Al_2O_3$ (AE-in, 2 nm) 0.26 mg; $Au/\delta$-$Al_2O_3$ (AE-ex, 2 nm) 0.35 mg; $Au/\gamma$-$Al_2O_3$ (CD-ex, 4 nm) 0.26 mg; $Au/\delta$-$Al_2O_3$ (AE-ex, 7 nm) 0.36 mg; $Au/\gamma$-$Al_2O_3$ (AE-0, 30 nm) 0.16 mg. Note that the plateaus correspond to full conversion of CO (a) or $O_2$ (b, d), thus the rates in these cases have no physical meaning.

**Table 2**
Turnover frequencies at 60 °C.

| Catalyst | TOF CO ox ($s^{-1}$) | TOF CO PrOx ($s^{-1}$) | TOF $H_2$ ox ($s^{-1}$) | TOF $H_2$ PrOx ($s^{-1}$) |
|---|---|---|---|---|
| $Au/TiO_2$ (reference) | 1.3 | 2.8 | 1.8 | 0.57 |
| $Au/\delta$-$Al_2O_3$ (2 nm) | 0.03 | 0.82 | 0.43 | 0.24 |
| $Au/\delta$-$Al_2O_3$ (7 nm)[a] | 0.02 | 0.15 | 0.08 | 0.12 |

[a] Obtained by heating of $Au/\delta$-$Al_2O_3$ (AE-ex, 2 nm) at 500 °C in air.

the order with respect to $H_2$ is 0.3 for CO PrOx, which is consistent with the previously reported values of 0.58 and 0.24, respectively, in the same conditions [11]. An even lower $H_2$ order (0.15 ± 0.1) for CO PrOx was found on $Au/TiO_2$ at 50 °C [15]. Along with the very low $H_2$ pressure (<0.5 kPa) needed to promote CO oxidation, this low value of the reaction order with respect to $H_2$ has been related to a "catalytic effect" of $H_2$ (see Section 4).

Reaction orders with respect to CO and $O_2$ are found equal to 0.4 and 0.3 in CO oxidation, and to 0.2 and 0.3 in CO PrOx, respectively, in agreement with the study of Calla and Davis on $Au/Al_2O_3$ [10]. More surprising is the positive value (0.55) found for the CO order

**Table 3**
Reaction orders for Au/δ-$Al_2O_3$ (AE-ex, 2 nm).

| Reaction | Temperature (°C) | Fixed pressure(s) (kPa) | Variable pressure (kPa) | CO order | $O_2$ order | $H_2$ order |
|---|---|---|---|---|---|---|
| CO ox | 100 | CO, $O_2$: 2 | CO, $O_2$: 0.5–4 | 0.40 ± 0.04 | 0.34 ± 0.02 | – |
| CO PrOx | 50 | CO, $O_2$: 2; $H_2$: 48 | CO, $O_2$: 0.5–4; $H_2$: 0.5–48 | 0.24 ± 0.03 | 0.32 ± 0.06 | 0.34 ± 0.04 |
| $H_2$ ox | 60 | $O_2$: 4; $H_2$: 48 | $O_2$: 0.5–4; $H_2$: 0.5–20 | – | 0.33 ± 0.01 | 0.53 ± 0.04 |
| $H_2$ PrOx | 100 | CO, $O_2$: 2; $H_2$: 48 | CO, $O_2$: 0.5–4; $H_2$: 0.5–48 | 0.55 ± 0.01 | 0.58 ± 0.12 | 0.66 ± 0.10 |

in $H_2$ PrOx, whereas CO addition is initially detrimental to $H_2$ oxidation (see Fig. 1b and d). This will be discussed in the next section.

Apparent activation energies ($E_a$) for independent CO and $H_2$ oxidations have been calculated from the data of Fig. 1. For most of the Au/$Al_2O_3$ catalysts, they vary in the 13–18 kJ/mol and 34–40 kJ/mol ranges for $H_2$-free CO oxidation and CO-free $H_2$ oxidation, respectively (see Fig. S2 for data plots); they reach 32 and 52 kJ/mol, respectively, for the catalyst with the largest particles (26 nm). In all cases however, the difference $\Delta E_a$(ox) between $E_a$($H_2$ ox) and $E_a$(CO ox) equals 22 ± 2 kJ/mol, irrespective of the catalyst. One may try to relate these results to the continuous decrease of the $CO_2$ selectivity in PrOx with temperature *and* to the nearly identical selectivity for all the catalysts (Fig. 1e). However, the values of $E_a$ under PrOx conditions are difficult to obtain due to high conversions in some cases (Fig. 1c and d), but $\Delta E_a$ can easily be calculated from the slope of the selectivity in an Arrhenius plot (see Fig. S3). This has been performed in the 20–120 °C range, where oxygen supply is not limiting: $\Delta E_a(\text{PrOx}) \equiv E_a(\text{H}_2\ \text{PrOx}) - E_a(\text{CO PrOx}) = 12 \pm 1$ kJ/mol. The large difference found between $\Delta E_a$(ox) and $\Delta E_a$(PrOx) illustrates well that in the co-presence of CO, $O_2$ and $H_2$, the mechanisms of CO and/or $H_2$ oxidations are not the same as they are under separate oxidation conditions, as we rationalize below.

## 4. Discussion

From our previous work on PrOx and on the basis of the present study, it has become obvious that gold-catalyzed CO oxidation does not proceed the same way whether hydrogen is present in the feed or not. The presence of hydrogen accelerates CO oxidation, which suggests a change in the reactive species, leading to specific mechanism and kinetics. The extent of this promotion is larger when the catalyst is highly active for hydrogen oxidation to water. We have previously shown that water is not the relevant intermediate and suggested that gold–hydroperoxy (Au–OOH) species may be the critical oxidizing ones [8,11,15,20]. However, the role of $H_2O$ in CO oxidation may be of a similar nature as that of $H_2$, $H_2O$ being likely to decompose and form OH or OOH adsorbates, although the energy barrier from $H_2 + O_2$ might be smaller, as already suggested in Ref. [15]. Several experiments have identified such intermediates in $H_2$ oxidation [17,18], PrOx [15,20] and propene/propane oxidation [26,27] over gold-based catalysts.

Fig. 2 schematizes an OOH-mediated reaction mechanism. The cycle on the right-hand side (R cycle) is based on the comprehensive study of $H_2$ oxidation on Au/$SiO_2$ by Barton and Podkolzin [17], who have theoretically predicted that $OOH^* + H_2 \rightarrow H_2O_2^* + H^*$ ($^*$denoting adsorbed state, here on Au) would be the rate-determining step for water formation. This catalytic cycle may prevail in our conditions ($CO + O_2 + H_2$) *at high temperature*, i.e. when CO PrOx becomes unselective. At low-temperature, selective oxidation of CO would be favoured according to the cycle on the left-hand side (L cycle). In this scheme, molecularly adsorbed $O_2$ is activated on Au by reaction with $H_2$, to form $OOH^*$ and $H^*$ species. Unlike the schemes proposed by Kung et al. for $H_2O/H_2$-induced regeneration [28] or by Daté et al. for water-promoted CO oxidation [12], this mechanism does not require $O_2$ dissociation on Au, which is known

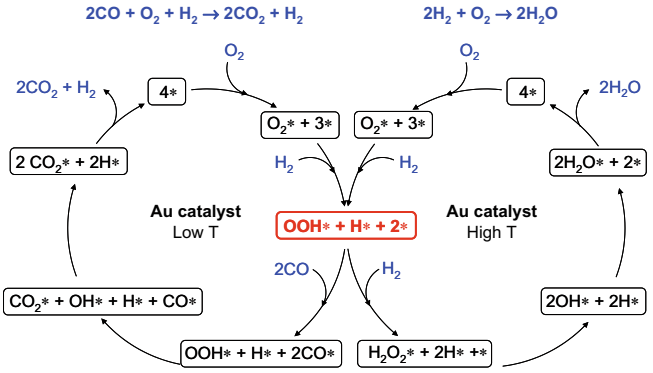


**Fig. 2.** Mechanistic scheme for CO oxidation in the presence of $H_2$ (CO PrOx, "L" cycle at the left) and $H_2$ oxidation ($H_2$ ox, "R" cycle at the right). Under PrOx conditions, the reaction continuously shifts from the R cycle to the L cycle as temperature decreases. * denotes adsorption site.

to be a highly activated step [5]. Hydrogen dissociation is easier than $O_2$ dissociation (and promoted by $O_2^*$ [29]) and $H^*$ stabilizes $O_2$ adsorption, thus favouring the formation of $OOH^*$ species on gold [19]. $CO^*$ and $OOH^*$ then convert to $CO_2$ and $OH^*$; $OH^*$ then reacts with $CO^*$ to produce $CO_2$ and $H^*$. The cycle is closed when the two $H^*$ recombine into $H_2$ or react with $O_2$ molecules to form new $OOH^*$ species. Density-functional-theory (DFT) calculations provide stability assessments and structural pictures for the various Au–$H_xO_y$ species [17,19,30].

Our previous study of PrOx over Au/$TiO_2$ by *operando* DRIFTS [15] allows us to get into more details concerning the possible nature of the intermediates and the active sites, so that the detailed mechanism schematized in Fig. 3 can be proposed. Note that the number of displayed steps in the catalytic cycle has been deliberately limited to facilitate its readability. As described above, $H_2$ dissociative adsorption and $O_2$ molecular adsorption on gold lead to $OOH^*$ species. For this step, an Eley–Rideal mechanism ($O_2^* + H_2 \rightarrow OOH^* + H^*$ [17] or $O_2 + H^* \rightarrow OOH^*$ [19]) cannot be excluded. Then, reaction of a gold–carbonyl (Au–CO) with the gold–hydroperoxide (Au–OOH) may involve a bicarbonate ($CO_2OH^*$) subsequently decomposing to a gold–hydroxyl (Au–OH) and a carboxylate ($CO_2^*$) adsorbed at the particle–support interface. All these species have been identified by DRIFTS, with the exception that Au–OH could not be distinguished from Au–OOH [15]. After $CO_2$ release, the second $CO^*$ involved in the cycle would react with $OH^*$ on gold to form $H^*$ and $CO_2^*$ via the hydroxycarbonyl intermediate proposed by Kung et al. [28]. Associative desorption of $H_2$ or $H^*$ reaction with $O_2$, and desorption of $CO_2$, would close the catalytic cycle. Noticeably, no "true" carbonates ($CO_3^*$) are involved in this cycle, in agreement with various works showing the disappearance of these poisoning species upon the addition of $H_2$ [13–15,28].

In the proposed schemes, $H_2$ is not consumed by the CO PrOx reaction. This explains why even a low amount of $H_2$ is sufficient to promote CO oxidation and why increasing this amount is only slightly beneficial to the reaction, as shown by the low (positive) value of the $H_2$ order. This mechanism is consistent with the above observation that a good $H_2$ oxidation catalyst is also a good PrOx

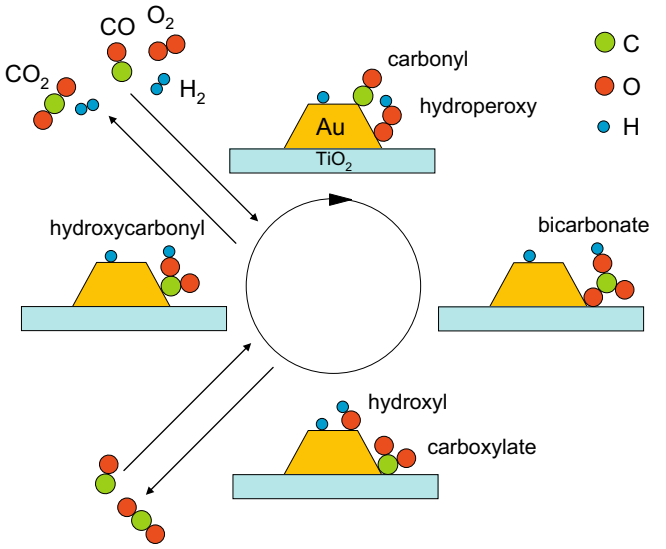


**Fig. 3.** Mechanistic scheme for $H_2$-promoted oxidation of CO (CO PrOx). This corresponds to a detailed picture of the cycle on the left-hand side of Fig. 2.

catalyst, with similar activities. In the present work on $Au/Al_2O_3$, this is the case for catalysts containing small gold nanoparticles (~2 nm).

As CO-free $H_2$ oxidation rate is significant for several catalysts in the low-temperature range (Fig. 1b), one may object that in the L cycle, $OH^*$ and $H^*$ can also react to form water, according to the R cycle. Explaining the actually high selectivity in CO PrOx at a low temperature by a simple kinetic competition between $CO^*$ and $H_2/H^*$ to react with $OOH^*/OH^*$ is not satisfactory. Indeed, it would not be consistent with the fact that oxygen consumption is faster in CO-free $H_2$ oxidation than in PrOx (within the 80–110 °C range in Fig. S4), showing that CO blocks, at least partially, $H_2O$-formation sites. Instead, let us assume that $OOH^*$ species may form on any gold sites, whereas the $OH^* + H^* \rightarrow H_2O$ reaction requires specific sites, e.g., low-coordination sites (LCS) like edges and corners. Indeed, Barton and Podkolzin have shown that this step is highly structure-sensitive (i.e., size-dependent) whereas the formation of $OOH^*$ species is much less sensitive to particle size [17]. Moreover, $CO^*$ is known to prefer LCS on gold [31,32]. Thus, if these sites are mainly occupied by CO, the formation of water is not favoured while that of $CO_2$ is possible via the L cycle. Indeed, a CO concentration as low as 0.5 mol.% appears to suppress the formation of water at 100 °C (Fig. S4). This supports the high $CO_2$ selectivity at low temperature *and* the observed negative effect of CO, consisting in the inhibition of $OH^* + H^*$ recombination to form water (Fig. 1b and d). However, as temperature increases, the CO desorption rate increases, thus more and more LCS become available for the $OH^* + H^* \rightarrow H_2O$ reaction. Consequently, the CO PrOx rate decreases and the $H_2$ PrOx rate increases (i.e., the $CO_2$ selectivity decreases, Fig. 1e). In other words, $H_2$ oxidation is less affected by the presence of CO at high temperature, as also shown by Fig. 1b and d. With this model, it is also possible to explain the positive CO order in $H_2$ PrOx (Table 3). LCS being already saturated by $CO^*$ at the lowest investigated CO concentration (0.5 mol.%, Fig. S4), increasing the CO pressure will especially accelerate the L cycle (positive order with respect to CO in CO PrOx) and thus lead to larger amounts of $OH^*$ and $H^*$. Even though the LCS are mainly blocked by $CO^*$, the probability of $OH^* + H^*$ reaction to water on the few available sites will increase. Finally, the size-dependency is well explained: smaller gold particles have proportionally more LCS, i.e., more active sites for CO adsorption and water formation, explaining the increased TOF with decreasing size for $H_2$ oxidation and PrOx.

## 5. Summary and conclusion

We have investigated the mechanism of PrOx by analyzing the effect of particle size on the kinetics of reactions involving $O_2$, CO and/or $H_2$ over $Au/Al_2O_3$ catalysts prepared by direct anionic exchange or colloidal deposition. Our main results are the following:

- Catalysts with small particles (~2 nm) exhibit the highest turnover frequencies for $H_2$ oxidation and PrOx. However, the selectivity to $CO_2$ is basically independent of particle size.
- The presence of hydrogen greatly promotes CO oxidation at low temperature whatever the particle size is, although the extent of this promotion is greater for catalysts with smaller particles.
- These results can be qualitatively explained by a PrOx mechanism that involves: (i) $H^*$, $OH^*$ and $OOH^*$ intermediates adsorbed on gold and bicarbonates, carboxylates and hydroxycarbonyls adsorbed on gold or at the particle–support interface (see catalytic cycles); (ii) low-coordination sites of the gold particles, the fraction of these sites increasing as particle size decreases.

In conclusion, we have shown that the $CO + O_2 + H_2$ system continuously switches from $H_2$ oxidation to CO oxidation as temperature decreases, with involvement of the same oxidizing intermediates. We hope that future theoretical works will provide some insights into the elementary steps suggested in our model, such as the $CO^* + OOH^*$ and $CO^* + OH^*$ reactions on gold.

## Acknowledgments

We thank IFP Lyon for E. Quinet's Ph.D. grant and financial support, D. Uzio (IFP) for his early contribution to this work and N. Cristin and P. Mascunan for ICP analysis. S. Ivanova, C. Petit and V. Pitchon from LMSPC (UMR CNRS 7515, Strasbourg, France) are gratefully acknowledged for their help in the catalyst preparation.

## Appendix A. Supplementary material

Supplementary data associated with this article can be found, in the online version, at doi:10.1016/j.jcat.2009.09.019.

## References

[1] D.T. Thompson, Nano Today 2 (2007) 40.
[2] P. Landon, J. Ferguson, B.E. Solsona, T. Garcia, S. Al-Sayari, A.F. Carley, A.A. Herzing, C.J. Kiely, M. Makkee, J.A. Moulijn, A. Overweg, S.E. Golunskie, G.J. Hutchings, J. Mater. Chem. 16 (2006) 199.
[3] M. Haruta, Gold Bull. 37 (2004) 27.
[4] A.S.K. Hashmi, G.J. Hutchings, Angew. Chem., Int. Ed. 45 (2006) 7896.
[5] G.C. Bond, C. Louis, D.T. Thompson (Eds.), Catalysis by Gold, Imperial Press, London, 2007.
[6] G. Ertl, Angew. Chem., Int. Ed. 47 (2008) 3524.
[7] A. Cho, Science 299 (2003) 1684.
[8] C. Rossignol, S. Arrii, F. Morfin, L. Piccolo, V. Caps, J.L. Rousset, J. Catal. 230 (2005) 476.
[9] S. Arrii, F. Morfin, A.J. Renouprez, J.L. Rousset, J. Am. Chem. Soc. 126 (2004) 1199.
[10] J.T. Calla, R.J. Davis, Ind. Eng. Chem. Res. 44 (2005) 5403.
[11] E. Quinet, F. Morfin, F. Diehl, P. Avenier, V. Caps, J.L. Rousset, Appl. Catal. B 80 (2008) 195.
[12] M. Daté, M. Okumora, S. Tsubota, M. Haruta, Angew. Chem., Int. Ed. 43 (2004) 2129.
[13] B. Schumacher, Y. Denkwitz, V. Plzak, M. Kinne, R.J. Behm, J. Catal. 224 (2004) 449.
[14] M. Azar, V. Caps, F. Morfin, J.L. Rousset, A. Piednoir, J.C. Bertolini, L. Piccolo, J. Catal. 239 (2006) 307.
[15] L. Piccolo, H. Daly, A. Valcarcel, F.C. Meunier, Appl. Catal. B 86 (2009) 190.
[16] H. Imai, M. Daté, S. Tsubota, Catal. Lett. 124 (2008) 68.
[17] D.G. Barton, S.G. Podkolzin, J. Phys. Chem. B 109 (2005) 2262.
[18] C. Sivadinarayana, T.V. Choudhary, L.L. Daemen, J. Eckert, D.W. Goodman, J. Am. Chem. Soc. 126 (2004) 38.
[19] L. Barrio, P. Liu, A. Rodriguez, J.M. Campos-Martin, J.L.G. Fierro, J. Phys. Chem. C 111 (2007) 19001.

[20] E. Quinet, L. Piccolo, H. Daly, F.C. Meunier, F. Morfin, A. Valcarcel, F. Diehl, P. Avenier, V. Caps, J.L. Rousset, Catal. Today 138 (2008) 43.
[21] S. Ivanova, C. Petit, V. Pitchon, Appl. Catal. A 267 (2004) 191.
[22] S. Biella, F. Porta, Prati, M. Rossi, Catal. Lett. 90 (2003) 23.
[23] M. Comotti, W.C. Li, B. Spliethoff, F. Schüth, J. Am. Chem. Soc. 128 (2006) 917.
[24] S. Ivanova, V. Pitchon, Y. Zimmermann, C. Petit, Appl. Catal. A 298 (2006) 57.
[25] F. Moreau, G.C. Bond, A.O. Taylor, J. Catal. 231 (2005) 105.
[26] J.J. Bravo-Suarez, K.K. Bando, J. Lu, M. Haruta, T. Fujitani, S.T. Oyama, J. Phys. Chem. C 112 (2008) 1115.
[27] J.J. Bravo-Suarez, K.K. Bando, T. Fujitani, S.T. Oyama, J. Catal. 257 (2008) 32.
[28] M.C. Kung, R.J. Davis, H.H. Kung, J. Phys. Chem. C 111 (2007) 11767.
[29] Naito, Tanimoto, J. Chem. Soc. Chem. Commun. (1988) 832.
[30] A. Bongiorno, U. Landman, Phys. Rev. Lett. 95 (2005) 106102.
[31] L. Piccolo, D. Loffreda, F.J.C.S. Aires, C. Deranlot, Y. Jugnet, P. Sautet, J.C. Bertolini, Surf. Sci. 566–568 (2004) 995.
[32] R. Meyer, C. Lemire, S.K. Shaikhutdinov, H.J. Freund, Gold Bull. 37 (2003) 72.